IEEE Access
Multidisciplinary | Rapid Review | Open Access Journal

Received September 1, 2020, accepted October 12, 2020, date of publication October 30, 2020, date of current version November 17, 2020.

Digital Object Identifier 10.1109/ACCESS.2020.3035005

Optimization of Full-Duplex Relaying System With Non-Linear Energy Harvester

SYED ADIL ABBAS KAZMI, (Member, IEEE), AND SINEM COLERI, (Senior Member, IEEE)
Department of Electrical and Electronics Engineering, Koç University, 34450 Istanbul, Turkey

Corresponding author: Sinem Coleri (scoleri@ku.edu.tr)

The work of Sinem Coleri was supported by the Scientific and Technological Research Council of Turkey under Grant #117E241.

ABSTRACT Simultaneous wireless information and power transfer (SWIPT) is a promising technique to prolong the lifetime of energy constrained relay-based systems. Most of the existing literature on relay-based SWIPT systems incorporate linear energy harvesting (EH) model. This article incorporates a non-linear EH model into the full-duplex (FD) amplify-and-forward (AF) relay-based system for the first time in the literature. We consider a practical non-linear energy harvester model namely constant-linear-constant (CLC) EH model, which takes into account the sensitivity and saturation characteristics of the EH circuit. First, the end-to-end outage probability of the system is derived for the time-switching (TS) based relay protocol. To prevent the outage performance degradation, the outage throughput and energy efficiency (EE) of the system is maximized by optimizing the TS parameter. Since the formulated problems are convex in nature, the golden-section method is used to find the optimal TS solution. Numerical results reveal the significance of employing a non-linear EH model by demonstrating the difference of the proposed model from the traditional linear EH model system and importance of using full-duplex relay by showing large performance gain over half-duplex relay-based (HDR) system, in terms of outage probability, throughput, and EE.

INDEX TERMS Amplify-and-forward (AF) relay, energy harvesting (EH), full-duplex (FD) system, outage probability.

I. INTRODUCTION

Beyond 5*th* generation (5G) wireless communication systems face huge challenges for high data rates, reliability, and energy efficiency of communication [1]. Cooperative relaying, where a source node transmits a data signal to the destination, a third node overhears it and relays the signal to the destination as well, is an efficient technique to provide reliable transmission, high throughput and long coverage [2], [3]. On the other hand, in recent years, energy harvesting (EH) from various renewable sources such as wind, solar, and radio frequency (RF) has been realized as a potential solution to prolong the lifetime of energy constrained communication networks [4]. Among these renewable sources, harvesting energy from the radio frequency (RF) is an efficient option for future wireless systems because of its controllability, reliability, and lower cost [5]. Since RF signals can carry both energy and information, simultaneous wireless information and power transfer (SWIPT), which is a combination of wireless information transfer and wireless power transfer (WPT) has received the great attention from the researchers recently [6]. In many applications of SWIPT, wireless powered relaying is one typical application scenario for cooperative systems, in which the energy constrained intermediate relay nodes rely on the harvested energy from RF signals of the source to assist its communication to the destination. There are two types of relay commonly being used, amplify-and-forward (AF) [8], where a relay node amplifies the received signal from the source and sends it to the destination and decode-and-forward (DF) [11], where a relay node first decodes the received signal and then sends it to the destination. For energy harvesting and information transmission, the relay nodes use two prominent architectures, namely, time-switching (TS) and power-splitting (PS) protocols [6], [7]. In TS-based SWIPT protocol, the relay harvests power from an energy signal sent by the source and receives the source transmitted information signal in two different time phases, whereas, in PS-based SWIPT, the received source signal is split into two signal streams to perform energy harvesting and information processing.

Initially, SWIPT-aided two-hop relaying systems incorporate half-duplex (HD) transmission and traditional linear

The associate editor coordinating the review of this manuscript and approving it for publication was Jenny Mahoney.

energy harvesting (EH) model [7]–[12]. The traditional linear EH model assumes that the output power of an energy harvester is linearly dependent on its input power. [7] derives the analytical expressions for the outage probability and ergodic capacity of an HD-AF relay-based system incorporating the TS and PS protocols, whereas [8] studies the system of [7] in the presence of interference at the relay and destination. In [9], the authors investigate the outage performance of an HD-AF relay-based system with PS protocol in the presence of a direct link between source and destination, whereas [10] incorporates the adaptive relaying (AR) protocol based on TS-PS protocol in HD-AF relay-based system. In [11], the authors derive the analytical expressions of the achievable throughput and ergodic capacity of an HD-DF relaying network for both TS and PS schemes. [12] studies an energy efficiency maximization (EEM) optimization problem for the multi-user multi-carrier energy-constrained HD-AF multi-relay network under the total source transmit power budget and energy-causality constraints. However, the limitation of the aforementioned relaying SWIPT systems to HD transmission results in loss of spectral efficiency. Therefore, full-duplex (FD) relaying, which utilizes the scarce frequency spectrum more efficiently by supporting simultaneous signal transmission and reception at the same frequency band, has been exploited.

FD relaying SWIPT systems with a linear EH model are investigated in [13]–[23]. The throughput of the FD-AF and DF relaying system based on a TS receiver structure is investigated in [13]. Later on, [14] extended the work of [13] to the FD multi-antenna system. In [15], the authors study the outage probability of the FD-DF relay system incorporating the PS protocol, whereas in [16] the outage probability and throughput of FD-AF relay system incorporating TS protocol are analyzed under the QoS constraints. [17] discusses the problem of relay selection in FD two-way communication system whereas, [18] analyzes the outage performance of four different energy harvesting schemes based on two-way communication FD relay system. [19] studies the outage performance for the SWIPT FD-EH relay system, with the relay node subjected to co-channel interference (CCI), under PS protocol. [20] analyzes the outage probability of the EH-based FD AF and DF relay system in α-μ environment, under TS protocol. [21] studies an FD-AF multiple relay system employing SWIPT receivers operating in interference channels under PS protocol and presents power allocation problem using game theory. [22] presents the problem of maximizing the energy efficiency of an FD-AF MIMO-OFDM system with self-energy recycling, whereas [23] analyzes an FD-AF MIMO relay system based on antenna switching with self energy recycling and presents the problem of maximizing the spectral efficiency. The above mentioned full-duplex systems are all based on the conventional linear EH model. As stated above, the linear EH model assumes that the output power of the energy harvester is linearly dependent on its input power. However, the components of the EH circuit in a real system are non-linear, and the traditional linear EH model is unrealistic. As a result, researchers start to study the practical non-linear EH models based on RF signals [24]–[45].

The non-linear EH model based on sigmoid function has been studied in [24]–[33], where as authors in [34]–[39] incorporates the non-linear EH model based on a linear-constant (LC) function. [40] studies the non-linear EH model based on a quadratic function and [41], [42] on a polynomial function obtained by a Taylor series expansion of the diode output in the rectifier. These non-linear EH models incorporate only the saturation effect of the EH circuit. Only recently, the authors in [43]–[45] incorporate the sensitivity characteristic [46] of the EH circuit in modeling non-linear models which is known as constant-linear-constant (CLC) model. Considering the sensitivity characteristic is important for EH circuits containing diodes.

The developed non-linear EH models are being used in the design and analysis of various SWIPT systems [27]–[33], [35]–[39], [42], [45]. For the non-linear EH model relay-based systems specifically, based on the sigmoid function [24], [32] study the PS scheme for the HD-AF relay-based system in the presence of a direct link between source and destination, where as [33] studies the resource allocation and relay selection in a two-hop AF relay-assisted HD multi-user orthogonal frequency division multiple access (OFDMA) network with PS scheme. Based on LC model, [35] calculates the outage capacity of the HD-AF relay system with TS protocol, whereas [36] deduces the expression of the secret outage probability in the HD multi-DF relay-based system with PS protocol. The outage probability of the HD-DF relay-based system incorporating PS protocol under the imperfect channel is presented in [37]. [38] studies the dynamic PS schemes for the HD-AF relay-based system under the perfect and imperfect channel scenario. In [39], the authors derive the expressions for the outage probability of the HD-DF relay system in the interference-limited environment. [43] studies the two way communication rate regions under fixed and mobile relays based on CLC function. However, the systems mentioned above are limited to HD mode of transmission. Authors in [45] study the outage performance and QoS optimization of a full-duplex relay system with a constant-linear-constant (CLC) energy harvesting model, considering both the finite sensitivity and saturation characteristics of the EH circuit. Based on the TS scheme, the authors incorporate the DF relay to co-operate between the source and destination.

Motivated by the previous works, this article incorporates a non-linear EH model into an FD-AF relay-based system for the first time in literature. We consider a practical CLC EH model, which takes into account both the sensitivity and saturation characteristics of the EH circuit [44], [45]. The main contributions of our work are as follows:

- We provide the analysis of the outage probability of an FD-AF relay-based system incorporating a non-linear constant-linear-constant (CLC) EH model, considering both the sensitivity and saturation characteristics of the EH circuit for the first time in the literature.

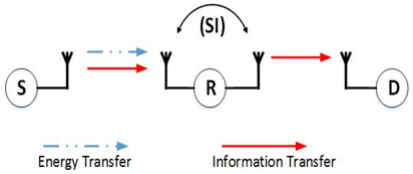

FIGURE 1. Full-duplex AF relay-based EH system.

- We optimize the TS scheme to maximize the system outage throughput and EE under the non-linear EH model. The formulated optimization problems are observed to be convex. Therefore, we exploit the golden-section method to find the optimal TS solution.
- The numerical results reveal that the performance of the proposed system under the non-linear EH model is different from the linear model system and illustrates the importance of using FD relay by showing significant performance gain over an HDR system incorporating both linear and non-linear EH models.

The rest of this article is organized as follows. Section II presents the system model and the non-linear energy harvesting model. In Section III, the outage probability analysis of an FD-AF relaying system is analyzed. Section IV and V present the optimization problems of maximizing the outage throughput and energy efficiency (EE) of the system and their solutions, whereas, in Section VI, numerical results are presented. Section VII concludes the paper.

II. SYSTEM MODEL

We consider a two-hop wireless communication system, where the information is transferred from the source node S to the destination node D, through an energy constrained intermediate relay node R, as shown in Fig. 1. Source and destination nodes are equipped with a single antenna, whereas relay contains two antennas (one receive antenna and one transmit antenna). We choose AF relay because of its following advantages. 1. Lower implementation and computational complexity. 2. Less delay at the relay terminal. 3. Transparent to the modulation/coding used by the source node. We assume that the AF relay operates in FD transmission mode and harvests energy from the source node. Due to the environmental limitations, we assume that there is no direct link between the source and destination, and communication can only be established via a cooperative relay node. We assume that the channel state information (CSI) is available to all the nodes. We obtain CSI by channel estimation in the training phase. First, the relay and destination transmit their own pilot signals, respectively. Hence, the CSI of source-relay link is obtained at the source, and CSI of relay-destination link is obtained at the relay. Then, the relay forwards CSI indicator to the source to indicate the CSI of relay-destination and self-interference link. Hence, CSI of all links in a two-hop FD relaying system is acquired at the source.

We assume that h_1 and h_2 denote the channel coefficients of the source-to-relay and relay-to-destination links, respectively, and h_R denotes the self-interference channel coefficient. The channels are quasi-static non-frequency selective Rayleigh fading, so the PDF and CDF of h_k ($k\epsilon(1), (2), (R)$) can be written as

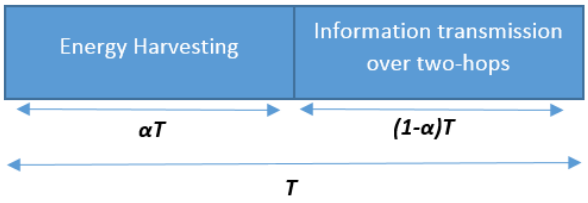

FIGURE 2. Block diagram of relay receiver architecture based on TS protocol.

$$f_{|h_k|^2}(x) = \frac{1}{\lambda_k} e^{-\frac{x}{\lambda_k}} \tag{1}$$

$$F_{|h_k|^2}(x) = 1 - e^{-\frac{x}{\lambda_k}} \tag{2}$$

where λ_k denotes the mean value of $|h_k|^2$.

A. TIME-SWITCHING (TS) PROTOCOL

Relay's receiver architecture is based on time-switching (TS) protocol [13], [14], [16]. The framework of TS is presented in Fig. 2, where the time slot T is divided into two phases, where the relay works in HD mode in the first time slot but FD mode in the second time slot. The first phase is of duration αT. This phase is used to transfer energy from the source to the relay. The second phase is of $(1-\alpha)T$ duration and is used to transfer the information from the source to the destination via a relay. The relay operates in FD mode in the second phase, i.e., receives the information from the source and transmits the information to the destination simultaneously. We consider a harvest-use strategy, where we assume that all the energy harvested by the relay in αT time fraction is used to transmit information to the destination in $(1-\alpha)T$ time fraction. For simplicity, we normalize the time period T to be equal to 1. We assume the usage of TS protocol because it outperforms PS protocol at low signal-to-noise-ratios and high transmission rates [7]. During the energy harvesting phase, the signal received at the relay at time t is

$$z_R(t) = h_1\sqrt{P_s}x_s(t) + n_R(t) \tag{3}$$

where P_s represents the transmission power at the source node, x_s is the normalized transmitted signal with $E(|x_s(t)|^2) = 1$ for all t, $n_R(t)$ is the additive white Gaussian noise at relay at time t, $CN \sim (0, \sigma_R^2)$.

During the information transmission phase, the signal received at the relay is

$$y_R(t) = h_1\sqrt{P_s}x_s(t) + h_R\sqrt{P_R}x_R(t) + n_R(t) \tag{4}$$

where $h_R\sqrt{P_R}x_R(t)$ is the self-interference signal due to the FD mode of the relay. After receiving the signal from the source node, the AF relay multiplies it with an amplification gain G_R and then forwards the signal to the destination. Hence, the signal at the destination at time t is given by

$$y_D(t) = h_2 G_R y_R(t) + n_D(t) \tag{5}$$

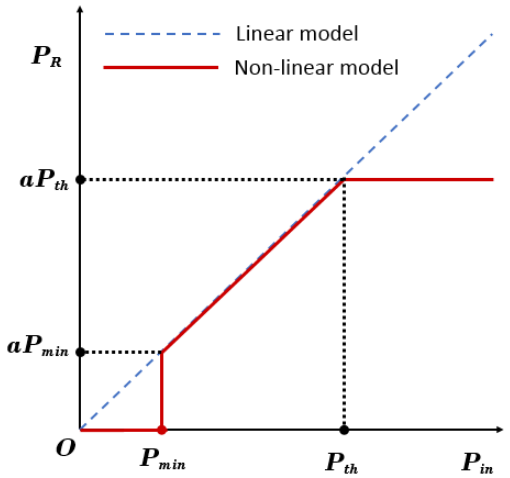

FIGURE 3. Constant-Linear-Constant (CLC) based non-linear EH model.

$$y_D(t) = h_2 G_R h_1 \sqrt{P_s} x_s(t) + h_2 G_R h_R \sqrt{P_R} x_R(t) + h_2 G_R n_R(t) + n_D(t) \tag{6}$$

where $n_D(t)$ is the additive white Gaussian noise at the destination at time t, $CN \sim (0, \sigma_D^2)$ and amplification factor G_R is expressed as

$$G_R = \sqrt{\frac{P_R}{P_s|h_1|^2 + P_R|h_R|^2 + \sigma_R^2}} \tag{7}$$

Considering Eqn. (6), the end-to-end signal-to-noise ratio SNR of the system, after some algebraic manipulations, can be express as in [47]

$$\gamma = \frac{P_s P_R |h_1|^2 |h_2|^2}{P_R^2 |h_2|^2 |h_R|^2 + P_R |h_R|^2 \sigma_D^2 + P_s |h_1|^2 \sigma_D^2} \tag{8}$$

The end-to-end rate of the system can be expressed as

$$R = (1-\alpha)\log_2(1+\gamma) \tag{9}$$

B. CONSTANT-LINEAR-CONSTANT (CLC) EH MODEL

In this work, we consider the non-linear EH model known as CLC. It takes into account the sensitivity and saturation characteristics of the EH circuit. Fig. 3 shows the harvested power for different input power values for two EH models, namely, linear EH model and CLC non-linear EH model [44], [45]. For the CLC EH model, when the input power is below the sensitivity value P_{min}, the EH circuit does not harvest any energy. When the input power becomes greater then P_{min}, the circuit operates in linear fashion but when it reaches the saturation value P_{th}, the output power of the harvester becomes constant.

Therefore, the transmission power of the relay can be expressed as

$$P_R = \begin{cases} 0, & P_s|h_1|^2 < P_{min} \\ \dfrac{\eta P_s |h_1|^2 \alpha}{1-\alpha}, & P_{min} \le P_s|h_1|^2 \le P_{th} \\ \dfrac{\eta P_{th} \alpha}{1-\alpha}, & P_s|h_1|^2 > P_{th} \end{cases} \tag{10}$$

where, η is the energy conversion efficiency. The existence of these three regions in the P_R expression results in three regions in SNR expressions. This is the main challenge we have to tackle in this study. Therefore, the end-to-end SNR can be expressed respectively as

$$\gamma = \begin{cases} 0, & P_s|h_1|^2 < P_{min} \\ \dfrac{P_s|h_1|^2|h_2|^2}{aP_s|h_1|^2|h_2|^2|h_R|^2 + |h_R|^2\sigma_D^2 + \frac{\sigma_D^2}{a}}, & P_{min} \le P_s|h_1|^2 \le P_{th} \\ \dfrac{P_s|h_1|^2|h_2|^2}{aP_{th}|h_2|^2|h_R|^2 + |h_R|^2\sigma_D^2 + \frac{P_s|h_1|^2\sigma_D^2}{aP_{th}}}, & P_s|h_1|^2 > P_{th} \end{cases} \tag{11}$$

where $a = (\frac{\eta\alpha}{1-\alpha})$.

III. OUTAGE ANALYSIS OF FD-AF RELAYING SYSTEM

An outage in the system happens when the rate is smaller than the target rate R_{th}. Therefore, outage probability can be defined as

$$P_{op} = Pr(R < R_{th}) = Pr(\gamma < \gamma_{th}) \tag{12}$$

where $\gamma_{th} = 2^{R_{th}} - 1$ represents the target SNR of the system. Considering the existence of three regions in the end-to-end SNR expressions of Eqn. (11) of the system, we can derive

$$P_{op} = 1 - I_1 - I_2 - I_3 \tag{13}$$

where

$$I_1 = Pr(\gamma > \gamma_{th}, P_s|h_1|^2 < P_{min}) \tag{14}$$
$$I_2 = Pr(\gamma > \gamma_{th}, P_{min} \le P_s|h_1|^2 \le P_{th}) \tag{15}$$
$$I_3 = Pr(\gamma > \gamma_{th}, P_s|h_1|^2 > P_{th}) \tag{16}$$

Now, we calculate I_1, I_2, and I_3 separately.

- $I_1 = Pr(\gamma > \gamma_{th}, P_s|h_1|^2 < P_{min})$

For the case of I_1, the input power $P_s|h_1|^2$ is below the sensitivity level P_{min}, the relay does not harvest energy, due to which information cannot be transferred to the destination. Hence $I_1 = 0$.

- $I_2 = Pr(\gamma > \gamma_{th}, P_{min} \le P_s|h_1|^2 \le P_{th})$

After some algebraic manipulations, I_2 in Eqn. (15) can be written as,

$$I_2 = Pr\Big(|h_1|^2 > C, A \le |h_1|^2 \le B\Big) \tag{17}$$

where $A = \frac{P_{min}}{P_s}$, $B = \frac{P_{th}}{P_s}$ *and* $C = \frac{\gamma th(|h_R|^2\sigma_D^2 + \frac{\sigma_D^2}{a^2})}{P_s|h_2|^2(1-a\gamma_{th}|h_R|^2)}$

We can divide I_2 into two further cases, namely when $C \le A$ and $A < C \le B$. Now, we solve for these two cases.

Case I: Note that when $C \le A$, Eqn. (17) becomes

$$I_{2.1} = Pr(C \le A, A \le |h_1|^2 \le B) \tag{18}$$

Putting the expressions of A,B, and C, and considering the fact that $|h_1|^2$ and $|h_2|^2$ are independent random variables, we can write $I_{2.1}$ as,

$$I_{2.1} = Pr\left(|h_2|^2 > \frac{\gamma_{th}(|h_R|^2\sigma_D^2 + \frac{\sigma_D^2}{a})}{(1 - a\gamma_{th}|h_R|^2)P_{min}}\right) Pr(A \leq |h_1|^2 \leq B) \tag{19}$$

$I_{2.1}$ can be further classified into two cases depending on the fact that $|h_2|^2$ is a positive value.

$$\begin{cases} Pr\left(|h_2|^2 < \frac{\gamma_{th}(|h_R|^2\sigma_D^2 + \frac{\sigma_D^2}{a})}{(1 - a\gamma_{th}|h_R|^2)P_{min}}\right), & |h_R|^2 < \frac{1}{a\gamma th} \\ Pr\left(|h_2|^2 > \frac{\gamma_{th}(|h_R|^2\sigma_D^2 + \frac{\sigma_D^2}{a})}{(1 - a\gamma_{th}|h_R|^2)P_{min}}\right) = 1, & |h_R|^2 > \frac{1}{a\gamma th} \end{cases} \tag{20}$$

Therefore, $I_{2.1}$ can be calculated as in Eqn. (21), as shown at the bottom of the page. After solving the integral in Eqn. (21) by standard integral evaluation method, we get

$$I_{2.1} = \left[\frac{1}{\lambda_R}\int_0^{\frac{1}{a\gamma_{th}}} e^{-\left(\frac{\gamma_{th}(x\sigma_D^2 + \frac{\sigma_D^2}{a})}{(1-a\gamma_{th}x)P_{min}\lambda_2} + \frac{x}{\lambda_R}\right)} dx\right] \times [F_{|h_1|^2}(B) - F_{|h_1|^2}(A)] \tag{22}$$

Since, there is no closed-form expression for the integral $\frac{1}{\lambda_R}\int_0^{\frac{1}{a\gamma_{th}}} e^{-\left(\frac{\gamma_{th}(x\sigma_D^2 + \frac{\sigma_D^2}{a})}{(1-a\gamma_{th}x)P_{min}\lambda_2} + \frac{x}{\lambda_R}\right)} dx$, we employ Gaussian-Chebyshev quadrature [49] to achieve an approximation of $I_{2.1}$ as

$$I_{2.1} \approx \left[\frac{\pi}{2\lambda_R a\gamma_{th}N}\sum_{n=1}^{N}\sqrt{1-a_n}f(b_n)\right]\left[e^{-\frac{A}{\lambda_1}} - e^{-\frac{B}{\lambda_1}}\right] \tag{23}$$

where N is a parameter that determines the trade off between complexity and accuracy, $a_n = cos\frac{2n-1}{2N}\pi$, and $b_n = \frac{1}{2a\gamma_{th}}[a_n + 1]$.

Case II: When $A < C \leq B$, I_2 becomes

$$I_{2.2} = Pr(A < C \leq B, C \leq |h_1|^2 \leq B) \tag{24}$$

Putting the expressions for A, B and C, and after some algebraic manipulations, we can write $I_{2.2}$ as in Eqn. (25), as shown at the bottom of the page. We can further classify $I_{2.2}$ on the basis of the value of random variable $|h_R|^2$ as

$$\begin{cases} \int_0^{\frac{1}{a\gamma_{th}}}\left\{\int_F^G\int_E^B f_{|h_1|^2}(x)f_{|h_2|^2}(y)dxdy\right\}f_{|h_R|^2}(z)dz, & |h_R|^2 < \frac{1}{a\gamma th} \\ 0, & |h_R|^2 > \frac{1}{a\gamma th} \end{cases} \tag{26}$$

Therefore, $I_{2.2}$ can be written as

$$I_{2.2} = \int_0^{\frac{1}{a\gamma_{th}}}\left\{\int_F^G\int_E^B f_{|h_1|^2}(x)f_{|h_2|^2}(y)dxdy\right\}f_{|h_R|^2}(z)dz \tag{27}$$

where $E = \frac{\gamma_{th}\left(|h_R|^2\sigma_D^2 + \frac{\sigma_D^2}{a}\right)}{P_{sy}\left(1-a\gamma_{th}|h_R|^2\right)}$, $F = \frac{\gamma_{th}\left(|h_R|^2\sigma_D^2 + \frac{\sigma_D^2}{a}\right)}{P_{th}\left(1-a\gamma_{th}|h_R|^2\right)}$, $G = \frac{\gamma_{th}\left(|h_R|^2\sigma_D^2 + \frac{\sigma_D^2}{a}\right)}{P_{min}\left(1-a\gamma_{th}|h_R|^2\right)}$ and $\left\{\int_F^G\int_E^B f_{|h_1|^2}(x)f_{|h_2|^2}(y)dxdy\right\}$ is the joint CDF of $|h_1|^2$ and $|h_2|^2$. The integral in Eqn. (27) can be solved by incorporating Gaussian-Chebyshev quadrature approximation. After solving, we get Eqn. (28), as shown at the bottom of the page. Since, the Gaussian approximation lies inside the integral in Eqn. (28), we can not find the final closed-form approximation without integral.

- $I_3 = Pr(\gamma > \gamma_{th}, P_s|h_1|^2 > P_{th})$

For the case of I_3, when the input power $P_S|h_1|^2$ is greater than the threshold level P_{th}, putting the expression for γ, and after some algebraic manipulations, Eqn. (16) becomes

$$I_3 = Pr(|h_1|^2 > D, |h_1|^2 > B) \tag{29}$$

$$I_{2.1} = \left\{1 - \left[\int_0^{\frac{1}{a\gamma_{th}}} F_{|h_2|^2}\left(\frac{\gamma_{th}(x\sigma_D^2 + \frac{\sigma_D^2}{a})}{(1 - a\gamma_{th}x)P_{min}}\right)f_{|h_R|^2}(x)dx + \int_{\frac{1}{a\gamma_{th}}}^{\infty} f_{|h_R|^2}(x)dx\right]\right\}\left[F_{|h_1|^2}(B) - F_{|h_1|^2}(A)\right] \tag{21}$$

$$I_{2.2} = Pr\left(\frac{\gamma th(|h_R|^2\sigma_D^2 + \frac{\sigma_D^2}{a})}{P_s|h_2|^2(1 - a\gamma_{th}|h_R|^2)} < |h_1|^2 \leq B, \frac{\gamma th(|h_R|^2\sigma_D^2 + \frac{\sigma_D^2}{a})}{(1 - a\gamma_{th}|h_R|^2)P_{th}} \leq |h_2|^2 \leq \frac{\gamma th(|h_R|^2\sigma_D^2 + \frac{\sigma_D^2}{a})}{(1 - a\gamma_{th}|h_R|^2)P_{min}}\right) \tag{25}$$

$$I_{2.2} \approx e^{-\frac{B}{\lambda_1}}\left[\frac{-\pi}{2\lambda_R a\gamma_{th}N}\sum_{n=1}^{N}\sqrt{1-a_n}f_1(b_n) + \frac{\pi}{2\lambda_R a\gamma_{th}N}\sum_{n=1}^{N}\sqrt{1-a_n}f_2(b_n)\right] + \frac{1}{\lambda_2\lambda_R}\int_0^{\frac{1}{a\gamma_{th}}}\left((\frac{G-F}{2})\sum_{n=1}^{N}\frac{\pi}{N}\sqrt{1-a_n}f(b_n)\right)e^{-\frac{z}{\lambda_R}}dz \tag{28}$$

where

$$D = \left(\frac{\gamma_{th}(aP_{th}^2|h_2|^2|h_R|^2 + |h_R|^2\sigma_D^2)}{P_s\left(|h_2|^2 - \frac{\gamma_{th}\sigma_D^2}{aP_{th}}\right)} \right).$$

We can further classify I_3 into two cases described below.

Case I : Note that when $D < B$, Eqn. (29) becomes

$$I_{3.1} = Pr(|h_1|^2 > B, D < B) \tag{30}$$

After incorporating the expressions of B and D and the fact that $|h_1|^2$ and $|h_R|^2$ are independent random variables, we can write $I_{3.1}$ as,

$$I_{3.1} = Pr(|h_1|^2 > B) Pr\left(|h_R|^2 < \frac{P_{th}(|h_2|^2 - \frac{\gamma_{th}\sigma_D^2}{aP_{th}})}{\gamma_{th}(aP_{th}|h_2|^2 + \sigma_D^2)}\right) \tag{31}$$

We can futher divide $I_{3.1}$ based on the fact that $|h_R|^2$ is a positive value.

$$\begin{cases} Pr\left(|h_R|^2 > \frac{P_{th}(|h_2|^2 - \frac{\gamma_{th}\sigma_D^2}{aP_{th}})}{\gamma_{th}(aP_{th}|h_2|^2 + \sigma_D^2)}\right) = 1, & |h_2|^2 < \frac{\gamma_{th}\sigma_D^2}{aP_{th}} \\ Pr\left(|h_R|^2 < \frac{P_{th}(|h_2|^2 - \frac{\gamma_{th}\sigma_D^2}{aP_{th}})}{\gamma_{th}(aP_{th}|h_2|^2 + \sigma_D^2)}\right), & |h_2|^2 > \frac{\gamma_{th}\sigma_D^2}{aP_{th}} \end{cases} \tag{32}$$

Therefore, we can write $I_{3.1}$ as Eqn. (33), as shown at the bottom of the page. After solving the integral in Eqn. (33) by using the standard integral evaluation method, we get

$$I_{3.1} = \left[1 - \frac{1}{\lambda_2}\int_{\frac{\gamma_{th}\sigma_D^2}{aP_{th}}}^{\infty} e^{-\left(\frac{P_{th}(x - \frac{\gamma_{th}\sigma_D^2}{aP_{th}})}{\gamma_{th}(aP_{th}x + \sigma_D^2)\lambda_R} + \frac{x}{\lambda_2}\right)} dx\right]\left[e^{-\frac{B}{\lambda_1}}\right] \tag{34}$$

Since there is no closed-form expression for the integral $\int_{\frac{\gamma_{th}\sigma_D^2}{aP_{th}}}^{\infty} e^{-\left(\frac{P_{th}(x - \frac{\gamma_{th}\sigma_D^2}{aP_{th}})}{\gamma_{th}(aP_{th}x + \sigma_D^2)\lambda_R} + \frac{x}{\lambda_2}\right)} dx$, and due to infinite limit, we can not approximate through Gaussian-Chebyshev quadrature.

Case II: When $D > B$, I_3 can be written as

$$I_{3.2} = Pr(|h_1|^2 > D, D > B) \tag{35}$$

After some algebraic manipulations, we can write $I_{3.2}$ as Eqn. (36), as shown at the bottom of the page. By observing Eqn. (36), we can further classify $I_{3.2}$ on the basis of $|h_2|^2$.

$$\begin{cases} 0, & |h_2|^2 < \frac{\gamma_{th}\sigma_D^2}{aP_{th}} \\ \int\limits_{\frac{\gamma_{th}\sigma_D^2}{aP_{th}}}^{\infty} \left\{ \int\limits_J^{\infty}\int\limits_I^{\infty} f_{|h_1|^2}(x) f_{|h_R|^2}(y) dxdy \right\} f_{|h_2|^2}(z) dz, & |h_2|^2 > \frac{\gamma_{th}\sigma_D^2}{aP_{th}} \end{cases} \tag{37}$$

Therefore, $I_{3.2}$ can be written as,

$$I_{3.2} = \int\limits_{\frac{\gamma_{th}\sigma_D^2}{aP_{th}}}^{\infty} \left\{ \int\limits_J^{\infty}\int\limits_I^{\infty} f_{|h_1|^2}(x) f_{|h_R|^2}(y) dxdy \right\} f_{|h_2|^2}(z) dz \tag{38}$$

where $I = \frac{\gamma_{th}\left(y\sigma_D^2 + yaP_{th}|h_2|^2\right)}{P_s\left(|h_2|^2 - \frac{\gamma_{th}\sigma_D^2}{aP_{th}}\right)}$, and $J = \frac{P_{th}\left(|h_2|^2 - \frac{\gamma_{th}\sigma_D^2}{aP_{th}}\right)}{\gamma_{th}\left(aP_{th}|h_2|^2 + \sigma_D^2\right)}$ and $\left\{ \int\limits_J^{\infty}\int\limits_I^{\infty} f_{|h_1|^2}(x) f_{|h_R|^2}(y) dxdy \right\}$ is the joint CDF of $|h_1|^2$ and $|h_R|^2$. After solving the integral,

$$I_{3.2} = e^{-\frac{B}{\lambda_1}} \int_{\frac{\gamma_{th}\sigma_D^2}{aP_{th}}}^{\infty} \frac{e^{-\left(\frac{P_{th}(z - \frac{\gamma_{th}\sigma_D^2}{aP_{th}})}{\gamma_{th}\lambda_R(aP_{th}z + \sigma_D^2)} + \frac{z}{\lambda_2}\right)}}{\left(\frac{\gamma_{th}\lambda_R(aP_{th}z + \sigma_D^2)}{(z - \frac{\gamma_{th}\sigma_D^2}{aP_{th}})P_s\lambda_1} + 1\right)} dz \tag{39}$$

Since there is no closed-form expression of the above integral and due to infinite limit, we can not find the approximation.

Finally, we can calculate outage probability P_{op} by calculating $I_{2.1}$ from Eqn. (23), $I_{2.2}$ from Eqn. (28), $I_{3.1}$ from Eqn. (34), and $I_{3.2}$ from Eqn. (39), and putting them into Eqn. (13).

IV. OUTAGE THROUGHPUT MAXIMIZATION PROBLEM

In this section, we maximize the end-to-end outage throughput of the FD-AF relaying system. The optimization problem can be expressed as [45]

$$\max_{\alpha} \; R = (1 - P_{op})(1 - \alpha)R_{th}$$

$$I_{3.1} = \left[\int\limits_0^{\frac{\gamma_{th}\sigma_D^2}{aP_{th}}} f_{|h_2|^2}(x)dx + \int\limits_{\frac{\gamma_{th}\sigma_D^2}{aP_{th}}}^{\infty} F_{|h_R|^2}\left(\frac{P_{th}(x - \frac{\gamma_{th}\sigma_D^2}{aP_{th}})}{\gamma_{th}(aP_{th}x + \sigma_D^2)}\right) f_{|h_2|^2}(x)dx \right]\left[1 - F_{|h_1|^2}(B)\right] \tag{33}$$

$$I_{3.2} = Pr\left(|h_1|^2 > \frac{\gamma_{th}(aP_{th}|h_2|^2|h_R|^2 + |h_R|^2\sigma_D^2)}{P_s\left(|h_2|^2 - \frac{\gamma th\sigma_D^2}{aP_{th}}\right)}, |h_R|^2 > \frac{P_{th}\left(|h_2|^2 - \frac{\gamma th\sigma_D^2}{aP_{th}}\right)}{\gamma_{th}(aP_{th}|h_2|^2 + \sigma_D^2)}\right) \tag{36}$$

$$s.t\ 0 \leq \alpha \leq 1 \tag{40}$$

where R_{th} is the target rate. We observe that the objective function of the problem (40) is concave w.r.t. α. Therefore, the problem is convex and the solution is unique. To find the optimal TS solution, we use line search method like golden-section method [48]. The optimization algorithm based on golden-section method is presented in Algorithm 1. The optimal maximum throughput algorithm based on golden-section method is described as follows. We first describe the interval to be searched $\alpha\epsilon$ [0, 1], accuracy to be achieved $\sigma = e^{-7}$, and golden-ratio $\epsilon = 0.618$. We then calculate α_o and $\tilde{\alpha_o}$ and throughput values $R(\alpha_o)$ and $R(\tilde{\alpha_o})$. Depending on the function values or whether the convergence criteria is fulfilled, we keep updating the interval until we get the optimal α.

Algorithm 1 Optimal Maximum Througput Algorithm

1. Initialization: $\epsilon = 0.618$, $a_o = 0$, $b_o = 1$, $k = 0$, $\sigma = e^{-7}$
2. $\alpha_o \leftarrow a_o + (1-\epsilon)(b_o - a_o)$
3. $\tilde{\alpha_o} = a_o + \epsilon(b_o - a_o)$
4. Calculate $R(\alpha_o)$ and $R(\tilde{\alpha_o})$
5. for $\forall k$ do
6. if $R(\alpha_o) > R(\tilde{\alpha_o})$ then
7. if $\mid \tilde{\alpha_k} - a_k \mid \leq \sigma$
8. $\alpha^*_{op} = \alpha_k$
9. Break
10. else
11. $a_{k+1} \leftarrow a_k, b_{k+1} \leftarrow \tilde{\alpha_k}, R(\alpha_{\tilde{k+1}}) \leftarrow R(\alpha_k)$
12. $\alpha_{\tilde{k+1}} \leftarrow \alpha_k$
13. $\alpha_{k+1} \leftarrow a_{k+1} + (1-\epsilon)(b_{k+1} - a_{k+1})$
14. Calculate $R(\alpha_{k+1})$
15. Continue
16. end if
17. else
18. if $\mid b_k - \alpha_k \mid \leq \sigma$ then
19. $\alpha^*_{op} \leftarrow \tilde{\alpha_k}$
20. Break
21. else
22. $a_{k+1} \leftarrow \alpha_k, b_{k+1} \leftarrow b_k, R(\alpha_{k+1}) \leftarrow R(\tilde{\alpha_k})$
23. $\alpha_{k+1} \leftarrow \tilde{\alpha_k}$
24. $\alpha_{\tilde{k+1}} \leftarrow a_{k+1} + \epsilon(b_{k+1} - a_{k+1})$
25. Calculate $R(\alpha_{\tilde{k+1}})$
26. Continue
27. end if
28. end if
29. end for
30. Return α^*_{op} and $R(\alpha^*_{op})$

The complexity of golden-section method is $\mathcal{O}(\log \frac{1}{\sigma})$, the number of iterations golden-section method takes to converge is $\left\lceil Clog\left(\frac{L}{\sigma}\right)\right\rceil$, where $C = (log(\frac{1}{\epsilon}))^{-1}$, L is the length of interval given by (b_o-a_o). In the golden search method, two function evaluations are made at the first iteration and then only one function evaluation is made for each subsequent iteration.

V. ENERGY EFFICIENCY (EE) MAXIMIZATION PROBLEM

In this section, we maximize the EE of the FD-AF relay-based EH system and find the optimal value of time fraction α. The EE of the system is given as

$$EE = \frac{R}{P_S} \tag{41}$$

The optimization problem is expressed below

$$\max_{\alpha}\ EE = \frac{(1-P_{op})(1-\alpha)R_{th}}{P_s}$$
$$s.t\ 0 \leq \alpha \leq 1 \tag{42}$$

where EE is the ratio of end-to-end outage throughput to the total consumed power in the system. We observe that the above problem is convex. To find the optimal solution, we use golden-section method similar to Algorithm 1.

VI. NUMERICAL RESULTS AND DISCUSSIONS

The goal of this section is to present the numerical results based on analytical expressions developed and verify the analysis through Monte-Carlo simulations. We assume that all the channels undergo Rayleigh fading. The attenuation in the channel is calculated by using both large scale and small scale fading. To model the large scale fading, following model is used.

$$PL(d, dB) = PL(d_0, dB) + 10\beta log_{10}\left(\frac{d}{d_0}\right) + Z \tag{43}$$

where, $PL(d, dB)$ is the path loss at distance d in dB, d_0 is the reference distance and path loss at reference distance $d_0 = 1m$ is taken as $70dB$, the term β is the path loss exponent and is taken as 3. Z is a zero mean Gaussian random variable with standard deviation $\sigma = 4$. For the simulations, unless otherwise specified, we set the parameters as follows [45]: We set the maximum transmit power of the source node to $P_s = 30$ dBm; energy conversion efficiency to $\eta = 0.7$; the sensitivity and saturation values of the EH circuit to $P_{min} = 17$ dBm and $P_{th} = 29$ dBm, respectively; noise variance to $\sigma_D^2 = \sigma_R^2 = \sigma^2 = 0.01$; target rate to $R_{th} = 3$bps/Hz; and the average channel gains $\lambda_1 = \lambda_2 = \lambda_i$ to 1. For convenience we define SNR $\gamma = \frac{P_s}{\sigma^2}$.

A. OUTAGE PROBABILITY AND THROUGHPUT VERSUS α FOR DIFFERENT SNR (γ)

Fig. 4 shows the outage probability for different values of time fraction α and for different SNR (γ). When we increase α, outage probability decreases, but when α reaches to a certain value, outage probability starts increasing. It is due to the trade-off of energy harvesting and information transmission phases. More specifically, when α increases, energy harvesting at relay increases which in turn increases the transmission power at the relay. Due to which, outage probability decreases to the minimum. However, when α keeps increasing, the

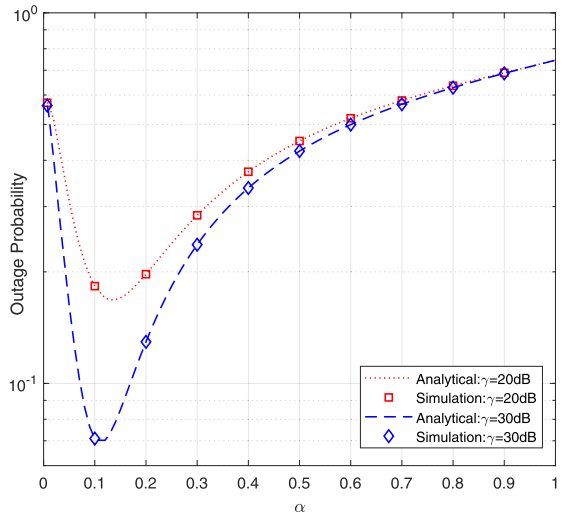

FIGURE 4. Outage probability for different values of time fraction α, where $\eta = 0.7$, $P_S = 30$ dBm.

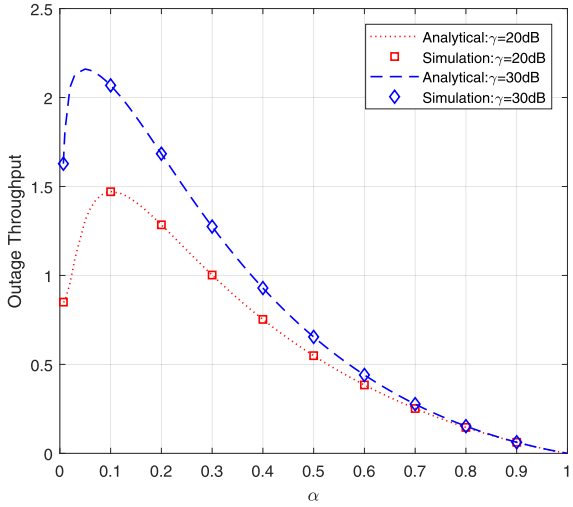

FIGURE 5. Outage throughput for different values of time fraction α, where $\eta = 0.7$, $P_S = 30$ dBm.

information processing time phase decreases which increases outage probability. It can be observed that high SNR achieves better performance as compared to low SNR.

Fig. 5 shows the outage throughput for different α values and for different γ. The outage throughput first increases and then decreases with increasing α. It is because of the trade-off of energy and information transmission phases. For high SNR value $\gamma = 30$ dB, the system achieves higher outage throughput as compared to $\gamma = 20$dB.

B. OUTAGE THROUGHPUT FOR DIFFERENT VALUES OF α UNDER DIFFERENT EH MODEL

Fig. 6 shows the outage throughput for different α and different EH models. The optimal α found for non-linear FD model is around 0.1, which is in accordance with the literature [45]. The optimal outage throughput in the non-linear FD model is smaller than that of a linear model. It is because of the

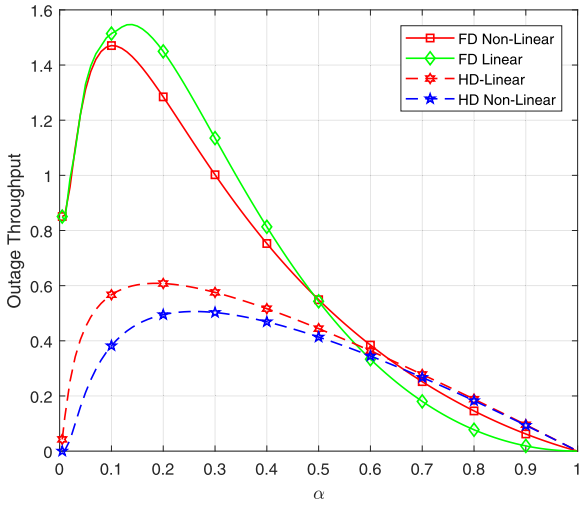

FIGURE 6. Outage throughput for different EH models, where $\sigma_D^2 = \sigma_R^2 = 0.01$, $\eta = 0.7$, $P_S = 30$ dBm.

non-linear behavior of the practical energy harvesting (EH) circuit, where we consider the sensitivity and saturation characteristics. It can be observed that the optimal α in a linear model is different from the one in non-linear and is not practical. When α reaches to a certain value, the outage throughput of the non-linear model becomes higher than the linear model, which is because of the saturation effect of the non-linear model. With increasing α, the transmission power of the relay keeps increasing in a linear model which means the self-interference keeps increasing and hence the throughput decreases. Due to saturation, the transmission power of the relay becomes constant in the non-linear model and so is the self-interference, therefore after a certain α, the throughput of the non-linear model becomes higher than the linear model. Moreover, it can be observed that FD system achieves better performance gain as compared to the HD system. In the HD system, the outage throughput of the non-linear model is smaller than the linear model, which is because, in the non-linear model, transmission power at the relay is limited and hence the outage probability in non-linear model is larger than the linear EH model system. Fig. 7 shows the outage throughput for different γ and different values of α. As γ increases, outage throughput first increases and then becomes steady. It is because of the saturation effect of the non-linear EH circuit. Specifically, as γ keeps increasing, the EH circuit saturates, and as a result, the outage throughput of the system becomes steady. It can be seen from the figure that optimal α achieves better throughput as compared to other α values.

C. COMPARISON OF LINEAR AND NON-LINEAR MODEL

Fig. 8 compares the proposed non-linear FD model with the linear model. We analyze our non-linear system on optimal time fraction (α^*) found from the linear model and plot the outage probability for different values of γ. It can be observed that by incorporating α^* of linear model, we achieve less throughput for a given (γ) as compared to the throughput we

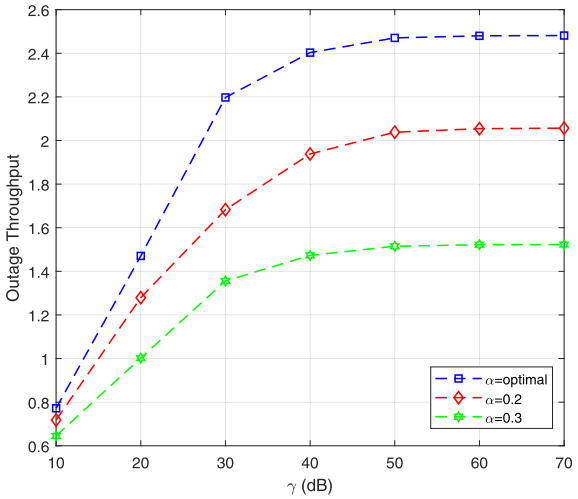

FIGURE 7. Outage Throughput for different SNR γ, where $\eta = 0.7$, $P_s = 30$ dBm.

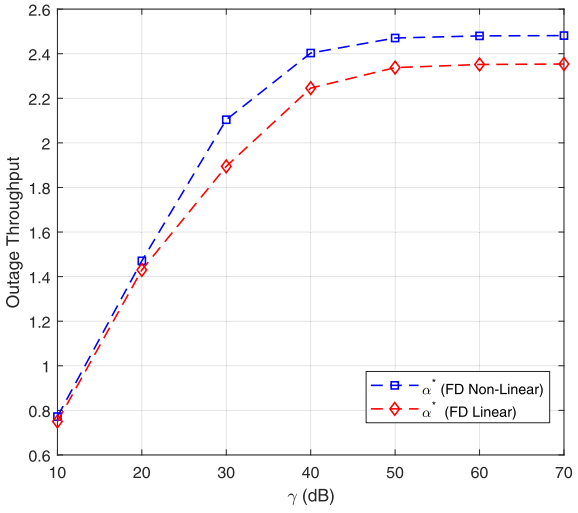

FIGURE 8. Outage Throughput for different values of SNR (γ) by incorporating optimal α* of linear model.

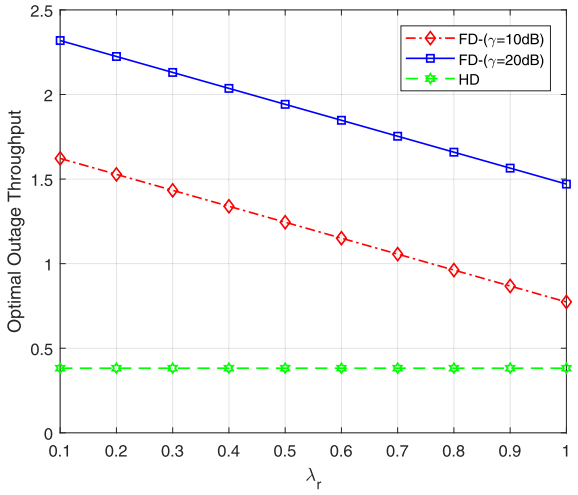

FIGURE 9. Outage throughput for different values of self-interference λ_R, where $\eta = 0.7$, $P_s = 30$ dBm.

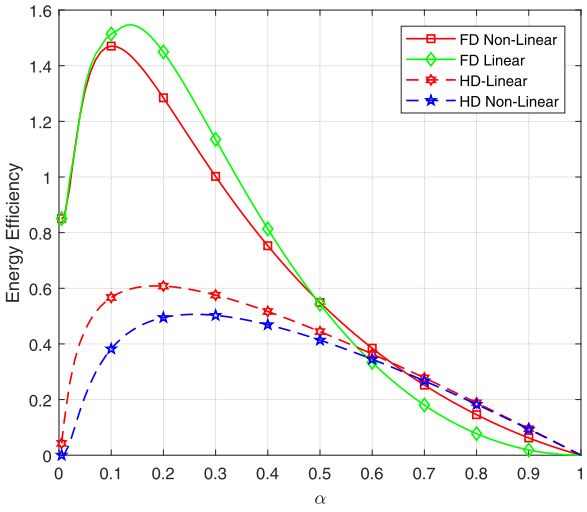

FIGURE 10. EE for different values of α and EH Models, where $\sigma_D^2 = \sigma_R^2 = 0.01$, $\eta = 0.7$, $P_s = 30$ dBm.

achieved on α^* of non-linear system. This result ensures the advantage and practicality of using the non-linear EH model over the linear EH model system.

D. OPTIMAL OUTAGE THROUGHPUT FOR DIFFERENT VALUES OF SELF-INTERFERENCE

Fig. 9 shows the optimal outage throughput versus self-interference λ_r of FD non-linear system with different values of γ and half-duplex non-linear system. As the strength of self-interference increases, outage throughput in the full-duplex system decreases. However, in a half-duplex system, there is no change in system performance. It is because self-interference does not exist in HD systems.

E. ENERGY EFFICIENCY FOR DIFFERENT VALUES OF α AND γ

Fig. 10 shows the energy efficiency (EE) for different values of α and different EH models. As observed for the outage throughput, the optimal EE in the non-linear FD model is different from that of a linear model. It is because of the non-linear behavior of the practical energy harvesting (EH) circuit, where we consider the sensitivity and saturation characteristics. The optimal α found for linear EH model is also different from the non-linear model, and is not practical. Moreover, FD system achieves better performance gain in terms of EE than the HD system. Fig. 11 shows EE for different values of γ and different α. It can be seen that as γ increases, energy efficiency of the system increases, but becomes steady as γ reaches to a certain value. It is because of the saturation characteristic of the EH circuit. It can be observed from the figure that optimal α gives better performance in terms of EE as compared to other arbitrary α values. We get similar results in Figs. 6 and 7 to Figs. 10 and 11, respectively, because of the value of P_s used in the simulations.

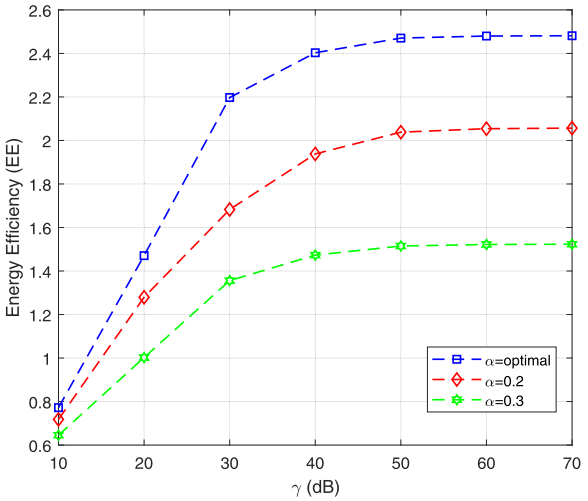

FIGURE 11. EE versus SNR γ for different α, where $\eta = 0.7$, $P_s = 30$ dBm.

VII. CONCLUSION AND FUTURE WORKS

This article presented a practical non-linear EH model, which takes into account the sensitivity and saturation characteristics of the EH circuit. Based on this model, we provided the outage probability analysis of an FD-AF relay-based system. To optimize the system performance, we presented an optimal solution of the TS parameter to maximize the outage throughput and EE of the system based on the golden-section method. Numerical results suggested that the proposed FD non-linear EH system outperforms the other existing systems including linear FD, linear and non-linear HD systems. This work can be further extended by incorporating power-splitting (PS) protocol, multi-antenna systems, Nakagami fading channels and more accurate non-linear EH models. Multi-antenna systems can be studied in the context of antenna-selection, and beamform designing for SWIPT. More accurate non-linear EH models can capture the increase in the received power between minimum threshold and saturation points by the use of a high-order polynomial and include the decrease in the received power after saturation.

REFERENCES

[1] E. Hossain and M. Hasan, "5G cellular: Key enabling technologies and research challenges," *IEEE Instrum. Meas. Mag.*, vol. 18, no. 3, pp. 11–21, Jun. 2015.

[2] E. C. Van Der Meulen, "Three-terminal communication channels," *Adv. Appl. Probab.*, vol. 3, no. 01, pp. 120–154, 1971.

[3] R. Pabst, B. H. Walke, D. C. Schultz, P. Herhold, H. Yanikomeroglu, S. Mukherjee, H. Viswanathan, M. Lott, W. Zirwas, M. Dohler, H. Aghvami, D. D. Falconer, and G. P. Fettweis, "Relay-based deployment concepts for wireless and mobile broadband radio," *IEEE Commun. Mag.*, vol. 42, no. 9, pp. 80–89, Sep. 2004, doi: 10.1109/MCOM.2004.1336724.

[4] S. Sudevalayam and P. Kulkarni, "Energy harvesting sensor nodes: Survey and implications," *IEEE Commun. Surveys Tuts.*, vol. 13, no. 3, pp. 443–461, 3rd Quart., 2011.

[5] M.-L. Ku, W. Li, Y. Chen, and K. J. Ray Liu, "Advances in energy harvesting communications: Past, present, and future challenges," *IEEE Commun. Surveys Tuts.*, vol. 18, no. 2, pp. 1384–1412, 2nd Quart., 2016.

[6] T. D. P. Perera, D. N. K. Jayakody, S. K. Sharma, S. Chatzinotas, and J. Li, "Simultaneous wireless information and power transfer (SWIPT): Recent advances and future challenges," *IEEE Commun. Surveys Tuts.*, vol. 20, no. 1, pp. 264–302, 1st Quart., 2018.

[7] A. A. Nasir, X. Zhou, S. Durrani, and R. A. Kennedy, "Relaying protocols for wireless energy harvesting and information processing," *IEEE Trans. Wireless Commun.*, vol. 12, no. 7, pp. 3622–3636, Jul. 2013.

[8] Y. Chen, "Energy-harvesting AF relaying in the presence of interference and Nakagami-*m* fading," *IEEE Trans. Wireless Commun.*, vol. 15, no. 2, pp. 1008–1017, Feb. 2016, doi: 10.1109/TWC.2015.2481393.

[9] H. Lee, C. Song, S.-H. Choi, and I. Lee, "Outage probability analysis and power splitter designs for SWIPT relaying systems with direct link," *IEEE Commun. Lett.*, vol. 21, no. 3, pp. 648–651, Mar. 2017.

[10] R. Tao, A. Salem, and K. A. Hamdi, "Adaptive relaying protocol for wireless power transfer and information processing," *IEEE Commun. Lett.*, vol. 20, no. 10, pp. 2027–2030, Oct. 2016.

[11] A. A. Nasir, X. Zhou, S. Durrani, and R. A. Kennedy, "Throughput and ergodic capacity of wireless energy harvesting based DF relaying network," in *Proc. IEEE Int. Conf. Commun. (ICC)*, Jun. 2014, pp. 4066–4071.

[12] A. Gupta, K. Singh, and M. Sellathurai, "Time-switching EH-based joint relay selection and resource allocation algorithms for multi-user multi-carrier AF relay networks," *IEEE Trans. Green Commun. Netw.*, vol. 3, no. 2, pp. 505–522, Jun. 2019, doi: 10.1109/TGCN.2019.2906616.

[13] C. Zhong, H. A. Suraweera, G. Zheng, I. Krikidis, and Z. Zhang, "Wireless information and power transfer with full duplex relaying," *IEEE Trans. Commun.*, vol. 62, no. 10, pp. 3447–3461, Oct. 2014.

[14] M. Mohammadi, B. K. Chalise, H. A. Suraweera, C. Zhong, G. Zheng, and I. Krikidis, "Throughput analysis and optimization of wireless-powered multiple antenna full-duplex relay systems," *IEEE Trans. Commun.*, vol. 64, no. 4, pp. 1769–1785, Apr. 2016.

[15] H. Liu, K. J. Kim, K. S. Kwak, and H. Vincent Poor, "Power splitting-based SWIPT with Decode-and-Forward full-duplex relaying," *IEEE Trans. Wireless Commun.*, vol. 15, no. 11, pp. 7561–7577, Nov. 2016.

[16] H. Liu, K. J. Kim, K. S. Kwak, and H. V. Poor, "QoS-constrained relay control for full-duplex relaying with SWIPT," *IEEE Trans. Wireless Commun.*, vol. 16, no. 5, pp. 2936–2949, May 2017.

[17] D. Wang, R. Zhang, X. Cheng, L. Yang, and C. Chen, "Relay selection in full-duplex energy-harvesting two-way relay networks," *IEEE Trans. Green Commun. Netw.*, vol. 1, no. 2, pp. 182–191, Jun. 2017.

[18] G. Chen, P. Xiao, J. R. Kelly, B. Li, and R. Tafazolli, "Full-duplex wireless-powered relay in two way cooperative networks," *IEEE Access*, vol. 5, pp. 1548–1558, Jan. 2017.

[19] J. Guo, S. Zhang, N. Zhao, and X. Wang, "Performance of SWIPT for full-duplex relay system with co-channel interference," *IEEE Trans. Veh. Technol.*, vol. 69, no. 2, pp. 2311–2315, Feb. 2020, doi: 10.1109/TVT.2019.2958626.

[20] G. Nauryzbayev, M. Abdallah, and K. M. Rabie, "Outage probability of the EH-based full-duplex AF and DF relaying systems in $\alpha - \mu$ environment," in *Proc. IEEE 88th Veh. Technol. Conf. (VTC-Fall)*, Chicago, IL, USA, Aug. 2018, pp. 1–6, doi: 10.1109/VTCFall.2018.8690985.

[21] Y. Liu, Z. Wen, N. C. Beaulieu, D. Liu, and X. Liu, "Power allocation for SWIPT in full-duplex AF relay interference channels using game theory," *IEEE Commun. Lett.*, vol. 24, no. 3, pp. 608–611, Mar. 2020, doi: 10.1109/LCOMM.2019.2963640.

[22] A. A. Nasir, H. D. Tuan, T. Q. Duong, and H. V. Poor, "Full-duplex MIMO-OFDM communication with self-energy recycling," Mar. 2019, *arXiv:1903.09931*. [Online]. Available: http://arxiv.org/abs/1903.09931

[23] C. Li, W. Wen, P. Wu, and M. Xia, "Wirelessly-powered full-duplex AF MIMO relay systems based on antenna switching," *IEEE Commun. Lett.*, vol. 23, no. 9, pp. 1640–1643, Sep. 2019, doi: 10.1109/LCOMM.2019.2924219.

[24] E. Boshkovska, D. W. K. Ng, N. Zlatanov, and R. Schober, "Practical non-linear energy harvesting model and resource allocation for SWIPT systems," *IEEE Commun. Lett.*, vol. 19, no. 12, pp. 2082–2085, Dec. 2015.

[25] E. Boshkovska, D. W. K. Ng, N. Zlatanov, A. Koelpin, and R. Schober, "Robust resource allocation for MIMO wireless powered communication networks based on a non-linear EH model," *IEEE Trans. Commun.*, vol. 65, no. 5, pp. 1984–1999, May 2017.

[26] R. Morsi, E. Boshkovska, E. Ramadan, D. W. K. Ng, and R. Schober, "On the performance of wireless powered communication with non-linear energy harvesting," in *Proc. IEEE 18th Int. Workshop Signal Process. Adv. Wireless Commun. (SPAWC)*, Sapporo, Japan, Jul. 2017, pp. 1–5.

[27] K. Xiong, B. Wang, and K. J. R. Liu, "Rate-energy region of SWIPT for MIMO broadcasting under nonlinear energy harvesting model," *IEEE Trans. Wireless Commun.*, vol. 16, no. 8, pp. 5147–5161, Aug. 2017.

[28] E. Boshkovska, X. Chen, L. Dai, D. W. K. Ng, and R. Schober, "Maxmin fair beamforming for SWIPT systems with non-linear EH model," in *Proc. IEEE 86th Veh. Technol. Conf. (VTC-Fall)*, Toronto, ON, Canada, Sep. 2017, pp. 1–6.
[29] J.-M. Kang, I.-M. Kim, and D. I. Kim, "Mode switching for SWIPT over fading channel with nonlinear energy harvesting," *IEEE Wireless Commun. Lett.*, vol. 6, no. 5, pp. 678–681, Oct. 2017.
[30] S. Wang, M. Xia, and Y.-C. Wu, "Space-time signal optimization for SWIPT: Linear versus nonlinear energy harvesting model," *IEEE Commun. Lett.*, vol. 22, no. 2, pp. 408–411, Feb. 2018.
[31] J.-M. Kang, I.-M. Kim, and D. I. Kim, "Wireless information and power transfer: Rate-energy tradeoff for nonlinear energy harvesting," *IEEE Trans. Wireless Commun.*, vol. 17, no. 3, pp. 1966–1981, Mar. 2018.
[32] X. Bai, J. Shao, J. Tian, and L. Shi, "Power-splitting scheme for nonlinear energy harvesting AF relaying with direct link," *Wireless Commun. Mobile Comput.*, vol. 2018, Jul. 2018, Art. no. 7906957.
[33] S. Gautam, E. Lagunas, S. Chatzinotas, and B. Ottersten, "Relay selection and resource allocation for SWIPT in multi-user OFDMA systems," *IEEE Trans. Wireless Commun.*, vol. 18, no. 5, pp. 2493–2508, May 2019.
[34] S. Pejoski, Z. Hadzi-Velkov, and R. Schober, "Optimal power and time allocation for WPCNs with piece-wise linear EH model," *IEEE Wireless Commun. Lett.*, vol. 7, no. 3, pp. 364–367, Jun. 2018.
[35] Y. J. Dong, M. J. Hossain, and J. L. Chen, "Performance of wireless powered amplify and forward relaying over Nakagami-mfading channels with nonlinear energy harvester," *IEEE Commun. Lett.*, vol. 20, no. 4, pp. 672–675, Apr. 2016.
[36] J.-L. Zhang, G.-F. Pan, and Y.-Y. Xie, "Secrecy outage performance for wireless-powered relaying systems with nonlinear energy harvesters," *Frontiers Inf. Technol. Electron. Eng.*, vol. 18, no. 2, pp. 246–252, Feb. 2017.
[37] J. Zhang and G. Pan, "Outage analysis of wireless-powered relaying MIMO systems with non-linear energy harvesters and imperfect CSI," *IEEE Access*, vol. 4, pp. 7046–7053, 2016.
[38] K. Wang, Y. Li, Y. Ye, and H. Zhang, "Dynamic power splitting schemes for non-linear EH relaying networks: Perfect and imperfect CSI," in *Proc. IEEE 86th Veh. Technol. Conf. (VTC-Fall)*, Sep. 2017, pp. 1–5.
[39] A. Cvetkovic and V. Blagojevic, "Performance analysis of nonlinear energy-harvesting DF relay system in interference limited Nakagami-*m* fading environment," *ETRI J.*, vol. 39, no. 6, pp. 803–812, Dec. 2017.
[40] X. Xu, A. Özçelikkale, T. McKelvey, and M. Viberg, "Simultaneous information and power transfer under a non-linear RF energy harvesting model," in *Proc. IEEE Int. Conf. Commun. Workshops (ICC Workshops)*, May 2017, pp. 179–184.
[41] B. Clerckx and E. Bayguzina, "Waveform design for wireless power transfer," *IEEE Trans. Signal Process.*, vol. 64, no. 23, pp. 6313–6328, Dec. 2016.
[42] B. Clerckx, "Wireless information and power transfer: Nonlinearity, waveform design, and rate-energy tradeoff," *IEEE Trans. Signal Process.*, vol. 66, no. 4, pp. 847–862, Feb. 2018.
[43] S. Wang, M. Xia, K. Huang, and Y.-C. Wu, "Wirelessly powered two way communication with nonlinear energy harvesting model: Rate regions under fixed and mobile relay," *IEEE Trans. Wireless Commun.*, vol. 16, no. 12, pp. 8190–8204, Dec. 2017.
[44] P. N. Alevizos and A. Bletsas, "Sensitive and nonlinear far-field RF energy harvesting in wireless communications," *IEEE Trans. Wireless Commun.*, vol. 17, no. 6, pp. 3670–3685, Jun. 2018.
[45] X. Xie, J. Chen, and Y. Fu, "Outage performance and QoS optimization in full-duplex system with non-linear energy harvesting model," *IEEE Access*, vol. 6, pp. 44281–44290, 2018, doi: 10.1109/ACCESS.2018.2861383.
[46] *PowerCast Module*. Accessed: Dec. 2016. [Online]. Available: http://www.mouser.com/ds/2/329/P2110B-Datasheet-Rev-3-1091766.pdf
[47] K. M. Rabie, B. Adebisi, and M. Alouini, "Half-duplex and full-duplex AF and DF relaying with energy-harvesting in log-normal fading," *IEEE Trans. Green Commun. Netw.*, vol. 1, no. 4, pp. 468–480, Dec. 2017, doi: 10.1109/TGCN.2017.2740258.
[48] W. Y. Yang, W. Cao, T.-S. Chung, and J. Morris, *Applied Numerical Methods Using MATLAB*. Hoboken, NJ, USA: Wiley, 2005.
[49] L. Shi, Y. Ye, R. Q. Hu, and H. Zhang, "System outage performance for three-step two-way energy harvesting DF relaying," *IEEE Trans. Veh. Technol.*, vol. 68, no. 4, pp. 3600–3612, Apr. 2019.

SYED ADIL ABBAS KAZMI (Member, IEEE) received the B.S. degree in electronics engineering from the NED University of Engineering and Technology, Pakistan, in 2012. He is currently pursuing the Ph.D. degree in electrical and electronics engineering with Koç University. He is also with the Wireless Networks Laboratory under the supervision of Prof. Sinem Coleri. His research interests include full-duplex wireless communications, simultaneous wireless information and power transfer, and non-linear energy harvesting networks.

SINEM COLERI (Senior Member, IEEE) received the B.S. degree in electrical and electronics engineering from Bilkent University, in 2000, and the M.S. and Ph.D. degrees in electrical engineering and computer sciences from the University of California at Berkeley, Berkeley, in 2002 and 2005, respectively. She was a Research Scientist with the Wireless Sensor Networks Berkeley Lab under the sponsorship of Pirelli and Telecom Italia, from 2006 to 2009. Since September 2009, she has been a Faculty Member with the Department of Electrical and Electronics Engineering, Koç University, where she is currently an Associate Professor. Her research interests include wireless communications and networking with applications in machine-to-machine communication, sensor networks, and intelligent transportation systems.

She received the Bilkent University Full Scholarship from Bilkent University, in 1995, the Regents Fellowship from the University of California at Berkeley, Berkeley, in 2000, the Marie Curie Reintegration Grant, in 2010, the Turk Telekom Collaborative Research Award, in 2011 and 2012, the Science Academy Young Scientist (BAGEP) Award, in 2014, the Turkish Academy of Sciences Distinguished Young Scientist (TUBA-GEBIP) and Turkish Academic Fellowship (TAF) Network - Outstanding Young Scientist Awards, in 2015, the IEEE COMMUNICATIONS LETTERS Exemplary Editor Award, the Science Heroes Association - Scientist of the Year Award, in 2016, the IEEE COMMUNICATIONS LETTERS Exemplary Editor Award, and the METU- Prof. Dr. Mustafa Parlar Foundation Research Encouragement Award, in 2017, the Outstanding Achievement Award in the Individual Awards Category by the Higher Education Council, in 2018, the IEEE COMMUNICATIONS LETTERS Exemplary Editor Award as an Area Editor, and the Outstanding Faculty Award from the College of Engineering, Koç University, in 2019. She has been an Editor of the IEEE TRANSACTIONS ON VEHICULAR TECHNOLOGY, since 2016, and of the IEEE TRANSACTIONS ON COMMUNICATIONS, since 2017, an Area Editor of the IEEE OPEN JOURNAL OF THE COMMUNICATIONS SOCIETY for Vehicular, Aerial and Satellite Communications and Networks since 2019, and an Area Editor of the IEEE COMMUNICATIONS LETTERS FOR WIRELESS NETWORKS—I, since 2019.